Molecular Cell, Vol. 12, 1379–1389, December, 2003, Copyright ©2003 by Cell Press

Structural Basis for Recruitment of the Adaptor Protein APS to the Activated Insulin Receptor

Junjie Hu,[1] Jun Liu,[2] Rodolfo Ghirlando,[3] Alan R. Saltiel,[2] and Stevan R. Hubbard[1,*]

[1]Skirball Institute of Biomolecular Medicine and Department of Pharmacology
New York University School of Medicine
New York, New York 10016
[2]Life Sciences Institute and Departments of Internal Medicine and Physiology
University of Michigan Medical Center
Ann Arbor, Michigan 48109
[3]National Institute of Diabetes and Digestive and Kidney Diseases
National Institutes of Health
Department of Health and Human Services
Bethesda, Maryland 20892

Summary

The adaptor protein APS is a substrate of the insulin receptor and couples receptor activation with phosphorylation of Cbl to facilitate glucose uptake. The interaction with the activated insulin receptor is mediated by the Src homology 2 (SH2) domain of APS. Here, we present the crystal structure of the APS SH2 domain in complex with the phosphorylated tyrosine kinase domain of the insulin receptor. The structure reveals a novel dimeric configuration of the APS SH2 domain, wherein the C-terminal half of each protomer is structurally divergent from conventional, monomeric SH2 domains. The APS SH2 dimer engages two kinase molecules, with pTyr-1158 of the kinase activation loop bound in the canonical phosphotyrosine binding pocket of the SH2 domain and a second phosphotyrosine, pTyr-1162, coordinated by two lysine residues in β strand D. This structure provides a molecular visualization of one of the initial downstream recruitment events following insulin activation of its dimeric receptor.

Introduction

Insulin stimulates glucose uptake in target cells by activating two distinct signaling pathways via its transmembrane receptor (Ebina et al., 1985; Ullrich et al., 1985), an $\alpha_2\beta_2$ glycoprotein and member of the receptor tyrosine kinase (RTK) family. One signaling pathway, mediated by phosphorylation of insulin receptor substrate (IRS) adaptor proteins (White, 1998), leads to activation of phosphatidylinositol 3-kinase (PI-3K) and subsequent activation of Akt/PKB (Shepherd et al., 1998). The second pathway culminates in activation of a Rho-family GTPase, TC10, through lipid-raft localization of a complex between Cbl, Cbl-associated protein, Crk, and the guanine nucleotide-exchange factor C3G (Chiang et al., 2001; Saltiel and Pessin, 2002). The integration of the outputs of these two signaling pathways to facilitate plasma membrane fusion of Glut4-containing vesicles is not well understood.

In the TC10 pathway, phosphorylation of Cbl by the insulin receptor is facilitated through recruitment of the adaptor protein APS to the receptor (Liu et al., 2002). APS, a member of a family of adaptor proteins that includes Lnk (Takaki et al., 1997) and SH2-B (Kotani et al., 1998; Nelms et al., 1999; Riedel et al., 1997), is an insulin receptor substrate expressed in skeletal muscle, heart, and adipose tissue (Ahmed et al., 1999; Moodie et al., 1999). These adaptor proteins possess a pleckstrin homology (PH) domain in the N-terminal half of the molecule, a Src homology 2 (SH2) domain in the C-terminal half, and polyproline stretches in the N- and C-terminal regions. Recruitment of APS to the insulin receptor results in phosphorylation of a carboxy-terminal tyrosine residue in APS, which then serves as a binding site for the SH2 domain of Cbl (Liu et al., 2002).

The interaction of APS with the insulin receptor is mediated by the SH2 domain. The SH2 domain is a well-characterized, typically monomeric, phosphotyrosine binding domain that recognizes phosphotyrosine in specific sequence contexts (Kuriyan and Cowburn, 1997). The APS SH2 domain interacts with the insulin receptor in a phosphorylation-dependent manner, and the site of interaction has been mapped to phosphotyrosines in the activation loop of the tyrosine kinase domain (Ahmed et al., 1999; Moodie et al., 1999). Phosphotyrosine recruitment sites in RTKs usually reside either N-terminal (juxtamembrane region) or C-terminal to the kinase domain. Moreover, a critical function of activation loop phosphorylation in most RTKs is stimulation of catalytic activity (Hubbard and Till, 2000). It is therefore intriguing that activation loop phosphotyrosines can also serve as recruitment sites for downstream signaling proteins.

To understand the molecular basis for recruitment of APS to the activated insulin receptor, we have determined the crystal structure of the APS SH2 domain in complex with the phosphorylated insulin receptor kinase domain (IRK). The structure reveals that the APS SH2 domain is arranged as a novel dimer, which will preferentially bind turn-containing phosphotyrosine segments, such as the phosphorylated activation loop of the insulin receptor. The APS SH2 dimer engages two IRK molecules by interacting with two phosphotyrosines in the activation loop, pTyr-1158 and pTyr-1162. Biochemical experiments in vitro and in cells confirm the dimeric nature of the APS SH2 domain and the importance of twin phosphotyrosine recognition in recruitment of APS to the two β subunits of the activated insulin receptor.

Results

Crystal Structure of the APS SH2 Domain

Based on sequence homology within the Lnk adaptor family and with other SH2 domains, an *E. coli* expression construct was engineered to encode APS residues 401–

*Correspondence: hubbard@saturn.med.nyu.edu

Table 1. Data Collection, Phasing, and Refinement Statistics

	APS(SH2)				APS(SH2)-IRK
Data collection					
Wavelength (Å)	0.9789	0.9793	0.9679	0.9872	1.1000
Resolution (Å)	30–2.3	30–2.3	30-2.3	30-2.3	30-2.6
Observations	75619	73678	76773	75788	156301
Unique reflections	19797	19849	19926	19788	32437
Completeness[a] (%)	96.4 (98.7)	96.5 (98.1)	96.9 (99.0)	96.2 (96.6)	99.8 (99.4)
R_{sym}[a,b] (%)	5.1 (18.3)	5.1 (18.2)	5.6 (21.0)	4.9 (19.2)	3.9 (16.4)
I/σI	20.2	20.2	15.7	16.5	22.4
Phasing[c]					
Figure of merit (overall, SOLVE)	0.60				
Figure of merit (overall, after RESOLVE)	0.69				
Refinement[d]					
Resolution (Å)	30-2.3				30-2.6
Reflections	10288				31461
R_{cryst}[e]/R_{free} (%)	22.4/25.5				23.3/27.9
Rmsd bond lengths (Å)	0.006				0.008
Rmsd bond angles (°)	1.2				1.5
Rmsd B factors[f] (Å^2) (main/side chain)	1.0/1.3				1.2/1.7
Average B factor (Å^2)	34.5				50.1

[a] Value in parentheses is for the highest resolution shell: 2.38–2.30 Å for APS(SH2) or 2.69–2.60 Å for APS(SH2)-IRK.
[b] $R_{sym} = 100 \times \Sigma|I - \langle I\rangle|/\Sigma I$.
[c] Phasing is based on two selenium sites in the asymmetric unit, one per APS SH2 protomer.
[d] Atomic model for APS(SH2) includes 1355 protein atoms, 2 sulfate ions, and 44 water molecules. Atomic model for APS(SH2)-IRK includes 5925 protein atoms, 262 bisubstrate inhibitor atoms, 2 Mn^{2+} ions, and 85 water molecules.
[e] $R_{cryst} = 100 \times \Sigma||F_o| - |F_c||/\Sigma |F_o|$, where F_o and F_c are the observed and calculated structure factors, respectively ($F_o > 0\sigma$). R_{free} determined from 5% of the data.
[f] For bonded protein atoms.

510 along with an N-terminal His-tag. Following cleavage of the His-tag by thrombin, purification by gel filtration chromatography showed two populations of the APS SH2 domain [APS(SH2)]. The predominant peak eluted at a position consistent with a dimer, whereas the second peak eluted later than would be predicted for a monomer (addressed below). MALDI-TOF mass spectrometry revealed that the dimer pool was enriched with an APS(SH2) protein lacking the C-terminal six residues, a consequence of thrombin digestion at a secondary site (after Arg-504). The dimer pool was used in cocrystallization trials with tris-phosphorylated IRK, in which the activation loop tyrosines, Tyr-1158/1162/1163, were phosphorylated. Crystals of the complex were obtained and an initial 3.3 Å data set was collected. The solvent content of the crystals was consistent with a 2:2 complex between APS(SH2) and IRK. The positions of the two IRK molecules in the asymmetric unit were determined by molecular replacement, but despite the use of several different SH2 domain search models, the two APS SH2 domains could not be placed.

To obtain independent phasing information for the APS SH2 dimer, we determined the crystal structure of selenomethionyl-containing APS(SH2) by multi-wavelength anomalous diffraction (MAD) (Hendrickson, 1991) and refined the structure at 2.3 Å resolution. Data collection and refinement statistics are given in Table 1.

The crystal structure of APS(SH2) reveals a novel dimeric arrangement of an SH2 domain (Figures 1A and 1B). For each of the two APS SH2 protomers (related by a noncrystallographic 2-fold axis), the N-terminal half of the molecule follows the canonical (monomeric) SH2 domain architecture, but the C-terminal half diverges significantly (Figure 1C). In a canonical SH2 domain, the N-terminal half comprises an α helix (αA) and a core β sheet of strands βA, βB, βC, and βD. The C-terminal half consists of a smaller β sheet (βD′, βE, and βF) followed by a second α helix (αB), the BG loop, and finally a short β strand (βG) that augments the core β sheet. In contrast, in the C-terminal half of the APS(SH2) structure, the five residues after βD are disordered, and the α helix that follows is approximately twice as long as the typical αB in an SH2 domain. This α helix in APS(SH2) includes residues that normally constitute βE and βF as well as αB (Figures 1C and 1D). In addition to its extra length, the C-terminal α helix in APS(SH2) is pivoted by 41° and translated by 8 Å compared to αB in a canonical SH2 domain (Figure 1C). The domain effectively ends with the C-terminal α helix.

The APS SH2 dimer interface is extensive, burying ~2400 Å^2 of total surface area. The extended C-terminal α helix of one protomer packs against the core β sheet and C-terminal α helix of the other protomer (Figure 1B). From the crystal structure and examination of SH2 domain sequences, the critical residue that mediates dimerization of APS(SH2) is Trp-475, which is buried in the center of the hydrophobic core of the dimer (Figure 1B). In a canonical SH2 domain, Trp-475 would be positioned in βF (βF2) (Figure 1D) (SH2 domain nomenclature taken from Eck et al., 1993) and be solvent exposed. Indeed, a hydrophilic residue predominates at this location in SH2 domains. Both APS and SH2-B contain tryp-

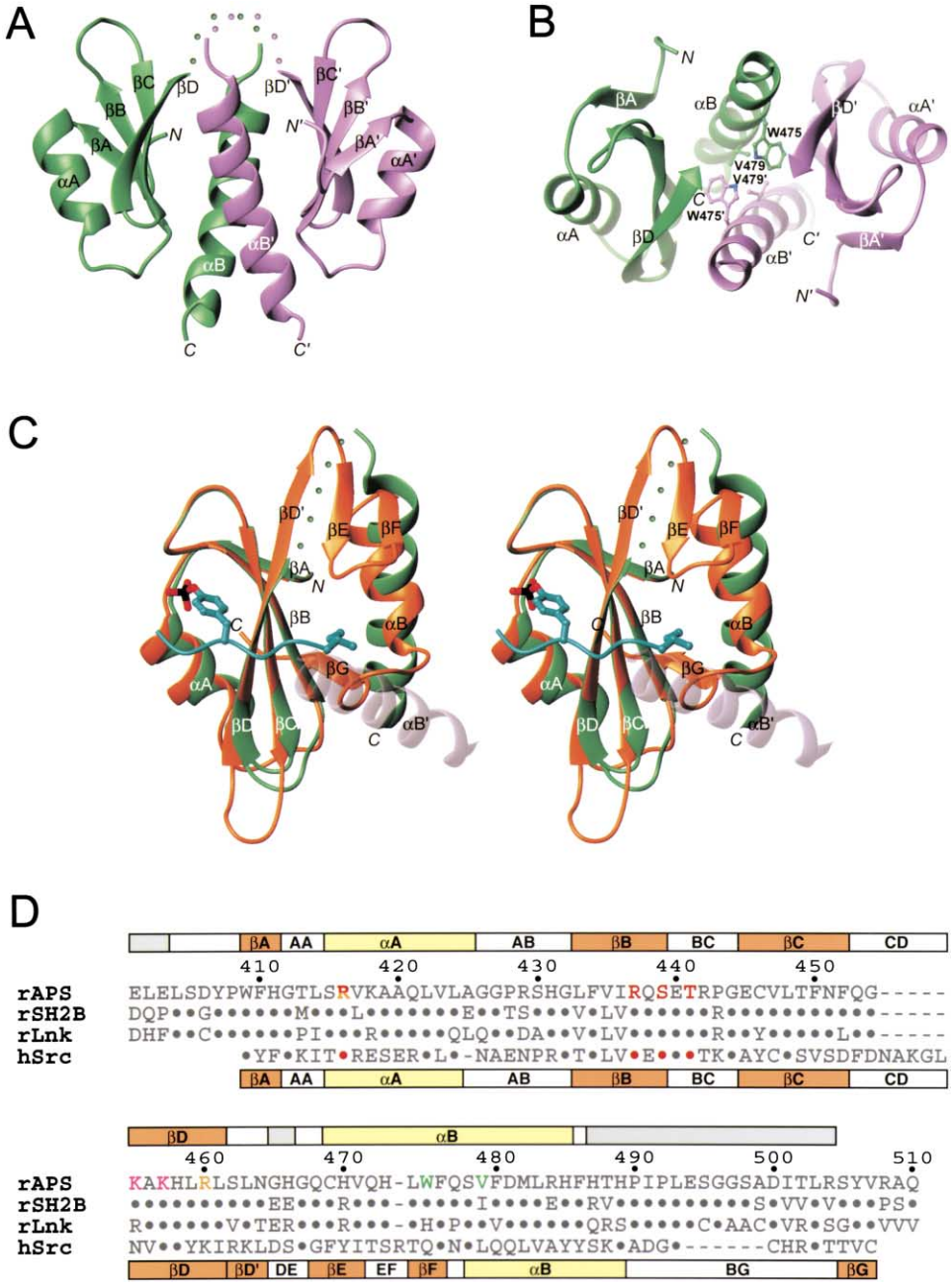

D

```
                βA  AA  αA      AB      βB      BC      βC      CD
                410     420     430     440     450
rAPS    ELELSDYPWFHGTLSRVKAAQLVLAGGPRSHGLFVIRQSETRPGECVLTFNFQG-----
rSH2B   DQP••G••••••M•••L•••••••E••TS•••V•LV••••••R••••••••••-----
rLnk    DHF••C••••••PI•••R•••••QLQ••DA••V•LV••••••R••Y•••••L••-----
hSrc    •YF•KIT•RESER•L•-NAENPR•T•LV•E•••TK•AYC•SVSDFDNAKGL
                βA  AA  αA      AB      βB      BC      βC      CD

                βD      αB
                460     470     480     490     500     510
rAPS    KAKHLRLSLNGHGQCHVQH-LWFQSVFDMLRHFHTHPIPLESGGSADITLRSYVRAQ
rSH2B   ••••••••••EE•••R•••-•••••I••••E••RV••••••••S•VV•V•••PS•
rLnk    R••••••V•TER•••R•••-•H•P••V••••••QRS•••••C•AAC•VR•SG••VVV
hSrc    NV••YKIRKLDS•GFYITSRTQ•N•LQQLVAYYSK•ADG•------CHR•TTVC
                βD  βD' DE  βE  EF  βF      αB          BG      βG
```

Figure 1. Crystal Structure of the APS SH2 Dimer

(A) Ribbon diagram of the APS SH2 dimer. The two protomers are colored green and purple, and the secondary structural elements for the second (purple) protomer are labeled with a prime symbol (′). The molecular 2-fold axis is vertical, and the N- and C termini for each protomer are indicated. There are five disordered residues between the end of βD and the beginning of αB, represented by small spheres.

(B) Trp-475 is a key determinant of APS(SH2) dimerization. View is from the top with respect to (A), with the molecular 2-fold axis perpendicular to the page. The side chains of Trp-475 and Val-479 in αB are shown in ball-and-stick representation.

(C) Stereo view of a superposition between the APS SH2 domain and the canonical Src SH2 domain. The core β sheets of the APS and Src (Waksman et al., 1993) SH2 domains were superimposed. The APS SH2 domain is colored green and the Src SH2 domain is colored orange. The pYEEI peptide cocrystallized with the Src SH2 domain is colored cyan, and the phosphotyrosine (P residue) and P+3 isoleucine are shown in ball-and-stick representation. Shown in purple (semitransparent) is αB from the other protomer (αB′) in the APS SH2 dimer, which is in position to interfere with binding of canonical phosphopeptide ligands.

(D) Comparative sequence alignment of Lnk family SH2 domains with the canonical Src SH2 domain. Shown are the SH2 domain sequences from rat APS, rat SH2-B, rat Lnk, and human Src. Residue numbering is for rat APS. Sequence identity with the rat APS SH2 domain is denoted by "•" and deletions are denoted by "-." Residues colored red in the APS and Src sequences coordinate the phosphotyrosine (pTyr-1158 for APS) in the canonical phosphotyrosine binding pocket, APS residues colored magenta coordinate pTyr-1162, residues colored orange are salt-bridged to aspartates in the IRK activation loop, and residues colored green are implicated in dimerization of the APS SH2 domain. Arg-416 is colored half red and half orange because it interacts with both pTyr-1158 and Asp-1161. Secondary structure assignments for the APS SH2 domain appear above the alignment and those for the canonical Src SH2 domain appear below the alignment. Gray regions in the secondary structure assignments for APS indicate disordered residues in the APS(SH2)-IRK crystal structure.

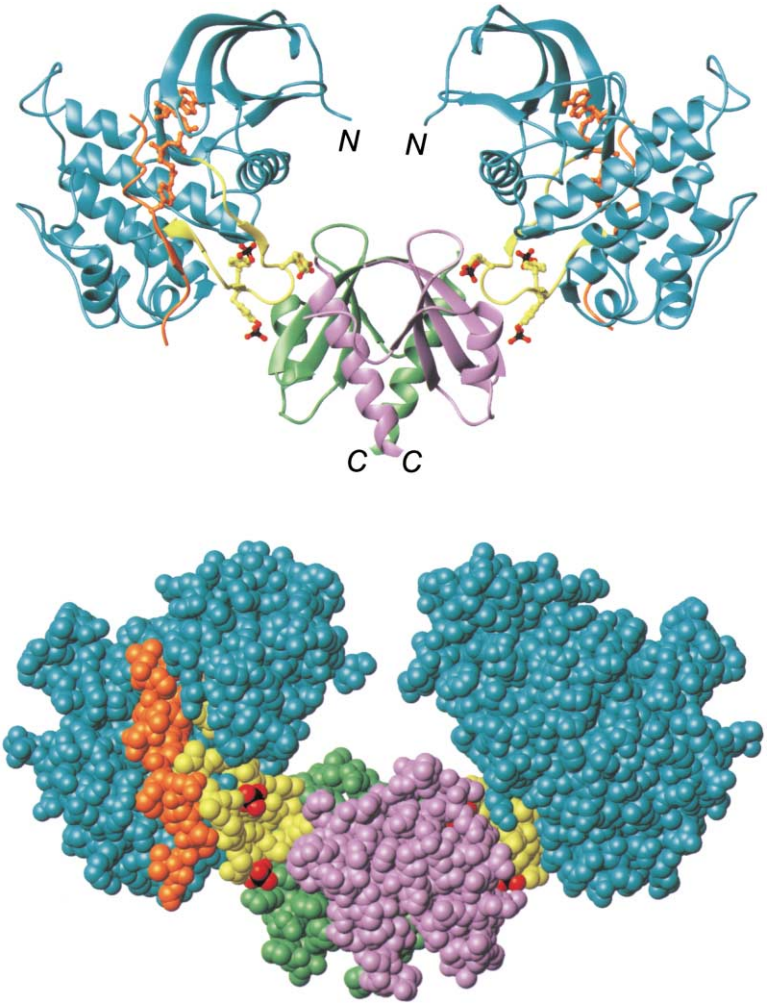

Figure 2. Crystal Structure of the APS(SH2)-IRK Complex

Ribbon diagram (top) and all-atom representation (bottom) of the APS(SH2)-IRK structure. The noncrystallographic 2-fold axis is vertical. The two IRK molecules are colored cyan, except for the activation loop, which is colored yellow. The two APS(SH2) protomers are colored green and purple. The three phosphotyrosine residues in the IRK activation loop are shown in ball-and-stick representation, with carbon atoms colored yellow, oxygen atoms colored red, and phosphorus atoms colored black. The bisubstrate inhibitor is colored orange, with the peptide portion shown in ribbon/coil representation, and the substrate tyrosine, linker, and ATPγS atoms shown in ball-and-stick representation. The N termini of the IRK molecules, which lead into the juxtamembrane region (34 residues to the transmembrane helix), are indicated, as are the C termini of the APS(SH2) protomers. The C-terminal tyrosine phosphorylation site in APS (Tyr-618) is 132 residues from the end of the SH2 domain.

tophan at this position, whereas Lnk, the other member of this adaptor family, contains histidine.

Previous structural studies have shown that phosphopeptides typically bind to an SH2 domain with an extended backbone conformation perpendicular to the core β sheet (Figure 1C), with pockets in the SH2 domain for engagement of phosphotyrosine (P residue) and the third residue C-terminal to phosphotyrosine (P+3 residue) (Kuriyan and Cowburn, 1997). A superposition of the APS SH2 dimer with the phosphopeptide-bound Src SH2 domain (Waksman et al., 1993) (Figure 1C) indicates that αB from the second protomer in the dimer will interfere with binding (to the first protomer) of a phosphopeptide with an extended backbone conformation. Evidently, one of the functional roles of APS(SH2) dimerization is to discriminate against canonical phosphotyrosine-containing sequences possessing a hydrophobic residue at the P+3 position, and to favor phosphopeptide segments that are predisposed to turn after the phosphotyrosine.

Crystal Structure of the Complex between the APS SH2 Dimer and IRK

The crystal structure of the complex between APS(SH2) and IRK was determined at 2.6 Å resolution by molecular replacement. The crystallographic statistics are given in Table 1. Cocrystallized with APS(SH2) and IRK was a bisubstrate inhibitor of IRK, which consists of ATPγS covalently linked to an 18-residue peptide substrate (Parang et al., 2001). Inclusion of the bisubstrate inhibitor improved the diffraction quality of the crystals, presumably by limiting the relative movements of the N- and C-terminal kinase lobes.

In the crystal structure of the complex, the APS SH2 dimer is centrally positioned with an IRK molecule bound to each of the two APS SH2 protomers, forming a 2:2 complex related by a noncrystallographic 2-fold axis (Figure 2). The interactions between APS(SH2) and IRK occur exclusively via the phosphorylated activation loop (Figure 3A). pTyr-1158 in the activation loop is bound in the canonical phosphate binding pocket of the SH2 domain, salt-bridged to invariant Arg-437 (βB5). Additional interactions with pTyr-1158 involve the side chains of Arg-416 (αA2), Ser-439 (βB7), and Thr-441 (BC2), as well as the backbone nitrogen of Glu-440 (BC1) (Figure 3A). This phosphotyrosine coordination is essentially equivalent to that observed between the Src or Lck SH2 domain and a high-affinity phosphopeptide (Waksman et al., 1993; Eck et al., 1993).

Significantly, the APS SH2 domain is observed to interact with a second phosphotyrosine in the IRK activation loop, pTyr-1162. Two lysines in βD of the SH2 do-

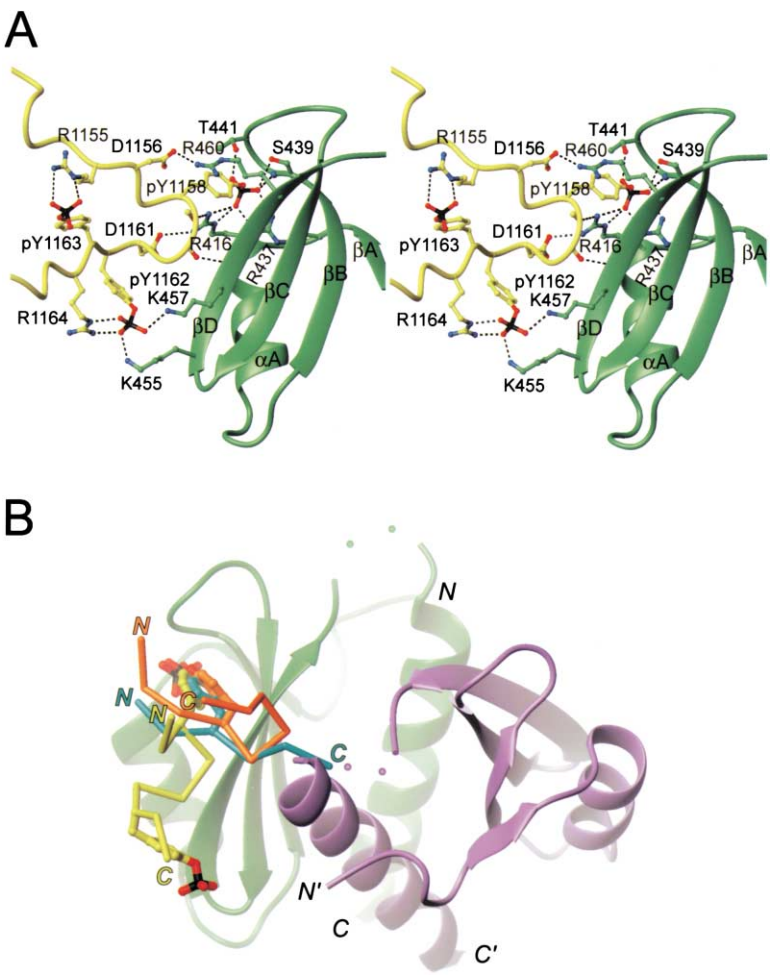

Figure 3. Mode of Binding of the IRK Activation Loop to the APS SH2 Domain

(A) Stereo view of the interactions between APS(SH2) and the IRK activation loop. The IRK activation loop is colored yellow and the APS SH2 protomer to which it binds is colored green. For clarity, the other APS SH2 protomer is not shown. Hydrogen bonds/salt bridges are shown with black dashed lines.

(B) Path of the IRK activation loop across the APS SH2 domain surface. A ribbon diagram of the APS SH2 dimer is shown, with the two protomers colored green and purple. The Cα trace of the IRK activation loop proximal to pTyr-1158 and pTyr-1162 is colored yellow, with the side chains of the two phosphotyrosines shown in ball-and-stick representation. The SH2 domains of Src (Waksman et al., 1993) and Grb2 (Rahuel et al., 1996) with bound peptides were superimposed (core β sheets) with the green APS SH2 protomer, and the phosphopeptides from the superposition, PQpYEEI for Src (cyan) and PSp YVNVQN for Grb2 (orange), are displayed as Cα traces, with the phosphotyrosines shown in ball-and-stick representation. The N- and C termini of the phosphopeptides are indicated by "N" and "C" of the appropriate color. The two disordered residues between βD and αB in the APS SH2 protomers are represented by small spheres.

main, Lys-455 (βD1) and Lys-457 (βD3), are salt-bridged to pTyr-1162, which is positioned by Arg-1164 in the activation loop for recognition by this lysine pair (Figure 3A). Both of these lysines are conserved in SH2-B and Grb10, adaptor proteins whose SH2 domains also bind to the IRK activation loop, although lysine or arginine is not uncommon at these positions in SH2 domains.

Several additional interactions between APS(SH2) and the activation loop, not directly involving the phosphotyrosines, are observed in the crystal structure (Figure 3A). Arg-416 (αA2), in addition to its interaction with the phosphate group of pTyr-1158, is also salt-bridged to Asp-1161 in the activation loop and is hydrogen-bonded to the backbone oxygen of pTyr-1158. Arg-460 (βD6) reaches over pTyr-1158 to engage Asp-1156 in the activation loop (Figure 3A). Thus, the interactions between the APS SH2 domain and the IRK activation loop are exclusively hydrophilic in character.

The path of the activation loop across the APS(SH2) surface differs substantially from that observed previously in SH2-phosphopeptide structures (Kuriyan and Cowburn, 1997). Rather than binding perpendicular to the strands of the core β sheet in APS(SH2), the IRK activation loop binds approximately in the plane of the β sheet (Figure 3B). The conformation of the tris-phosphorylated activation loop, including a tight turn just after pTyr-1158, is stabilized by numerous interactions within the kinase domain (Hubbard, 1997). This turn directs the polypeptide chain away from the steric block imposed by the extended C-terminal helix of the other protomer in the APS SH2 dimer, and positions pTyr-1162 for interaction with Lys-455 and Lys-457 in βD. Although a turn following the phosphotyrosine is common to both the IRK activation loop and pYxN sequences which bind to the Grb2 SH2 domain (Rahuel et al., 1996), the orientation of the turn with respect to the SH2 domain surface is markedly different (Figure 3B).

The bisubstrate inhibitor cocrystallized with IRK and APS(SH2) binds to IRK as observed previously (Parang et al., 2001) (Figure 2), with electron density for Mn•ATPγS, the linker segment, and 13 residues of the peptide substrate. A superposition of the structure of tris-phosphorylated IRK (with bisubstrate inhibitor bound) with the two IRK molecules in the APS(SH2)-IRK structure yields $<$0.8 Å rms deviation in Cα positions, indicating no significant change in the conformation of the kinase upon engaging the APS SH2 domain. Moreover, the activation loops with and without bound APS(SH2) superimpose to within 0.5 Å rms deviation (Cα positions).

Biochemical Studies of the APS SH2 Domain

The oligomerization properties of the SH2 domains of APS and SH2-B were analyzed by gel filtration chromatography (Figure 4A). Wild-type APS(SH2) elutes in two peaks, the first at a volume corresponding to a 26 kDa

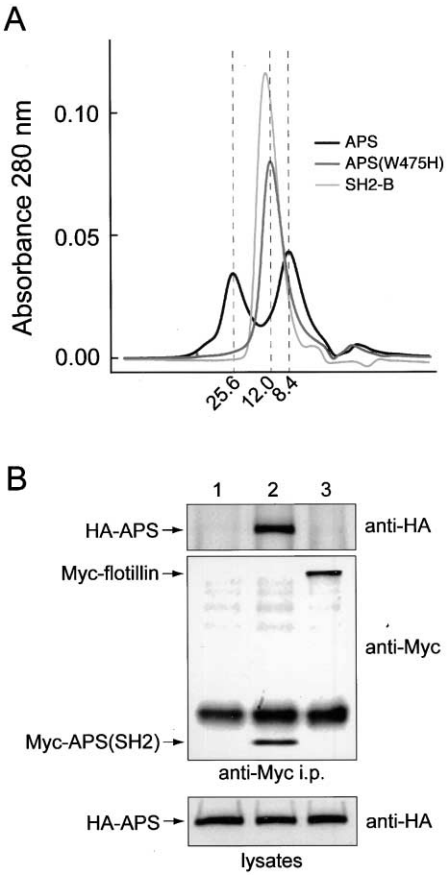

Figure 4. Biochemical Studies of the APS SH2 Domain

(A) Gel filtration study of the SH2 domains of APS and SH2-B. Wild-type APS(SH2) (black trace; residues 401–510 with His-tag; 200 μl at 85 μM), Trp-475→His APS(SH2) (dark gray trace; 170 μl at 100 μM), or the SH2 domain of SH2-B (light gray trace; 100 μl at 195 μM) were loaded onto a Superose-12 gel filtration column. The numbers along the abscissa are the corresponding molecular weights in kDa for the peaks (indicated by dashed vertical lines) in the elution profile. The column was calibrated using four protein standards: ribonuclease A (13.7 kDa), chymotrypsinogen A (25 kDa), ovalbumin (43 kDa), and albumin (67 kDa).

(B) Oligomerization of the APS SH2 domain in mammalian cells. COS-1 cells were cotransfected with HA-tagged, full-length APS and either empty vector (lane 1), Myc-tagged APS(SH2) (lane 2), or Myc-tagged flotillin (negative control for Myc tag). Cells were lysed and immunoprecipitated with an anti-Myc antibody. Immunoprecipitates (top two blots) were analyzed by Western blotting using antibodies to HA (top) or to Myc (bottom). The lysates were analyzed by Western blotting using antibodies to HA to show approximately equal amounts of HA-tagged, full-length APS (bottom blot). The identification of the bands appears on the left side of the blots.

protein, consistent with an APS SH2 dimer (calculated mass = 29.2 kDa), and the second at a volume corresponding to a protein of 8.4 kDa, significantly smaller than an APS SH2 monomer. In contrast to wild-type APS(SH2), the Trp-475→His mutant APS(SH2) and the SH2-B SH2 domain elute in single peaks at volumes consistent with well-behaved monomers. These data, in light of the crystal structure, suggest that the second peak of wild-type APS(SH2) is an aberrant monomer—possibly an individual protomer from the APS SH2 dimer. The Trp-475→His substitution converts the APS SH2 domain into a monomeric form that likely adopts the canonical SH2 domain architecture.

To provide evidence that the APS SH2 domain dimerizes in a cellular context, cotransfection experiments in mammalian cells were performed. Because of the likely existence of an N-terminal dimerization motif in APS (see Discussion), a Myc-tagged vector expressing just the APS SH2 domain and an HA-tagged vector expressing full-length APS were transiently transfected into COS-1 cells. Immunoprecipitation and Western blot analysis demonstrate that full-length APS associates with Myc-tagged APS(SH2) but not with a control Myc-tagged protein (Figure 4B).

Biochemical Studies of the Interaction between the APS SH2 Domain and IRK

To verify that Lys-455 (βD1) and Lys-457 (βD3), in addition to Arg-437 (βB5), are important in the recognition of the insulin receptor by the APS SH2 domain, mutations were introduced at these positions in full-length APS, and the wild-type and mutant proteins were transiently transfected into CHO-IR cells. The results of these experiments indicate that each of these basic residues in the APS SH2 domain contributes to the interaction with the activated insulin receptor (Figure 5A). Commensurate with the loss of interaction between the APS mutants and the insulin receptor, the mutants were not phosphorylated by the insulin receptor (Figure 5A). These mutations were also introduced into the isolated APS SH2 domain, and the binding to tris-phosphorylated IRK was studied by native gel-shift analysis. As with full-length APS, this experiment shows that Arg-437 and Lys-457 are critical for the interaction with IRK and, in addition, indicates that Lys-455 is less important than Lys-457 (Figure 5B). This latter result is consistent with the greater solvent exposure of Lys-455 versus Lys-457; Lys-457 is flanked by αB from the other protomer, which positions the lysine side chain for interaction with pTyr-1162.

The affinity of the interaction between APS(SH2) and tris-phosphorylated IRK was measured by sedimentation equilibrium. Sedimentation data for the carboxy-terminally truncated APS SH2 domain (residues 401–504) and for IRK indicate that, individually, both proteins are monodisperse with experimentally determined molecular masses consistent with an APS SH2 dimer and an IRK monomer. Sedimentation experiments on 2:1, 2:2, and 2:4 stoichiometric mixtures of APS(SH2) and IRK revealed the formation of higher order complexes. Best fits were obtained when data were analyzed in terms of formation of both 2:1 and 2:2 complexes (Figure 6), yielding a disassociation constant (K_d) of 110–420 nM for loading of the first IRK molecule onto the APS SH2 dimer, and a significantly higher disassociation constant of 27–160 μM for loading of the second IRK molecule onto the 2:1 APS(SH2):IRK complex. These data demonstrate that binding of IRK to the APS SH2 dimer is negatively cooperative.

Discussion

Signaling proteins with phosphotyrosine-recognition domains (SH2 or PTB) are typically recruited to an activated RTK by binding to phosphotyrosines (in particular

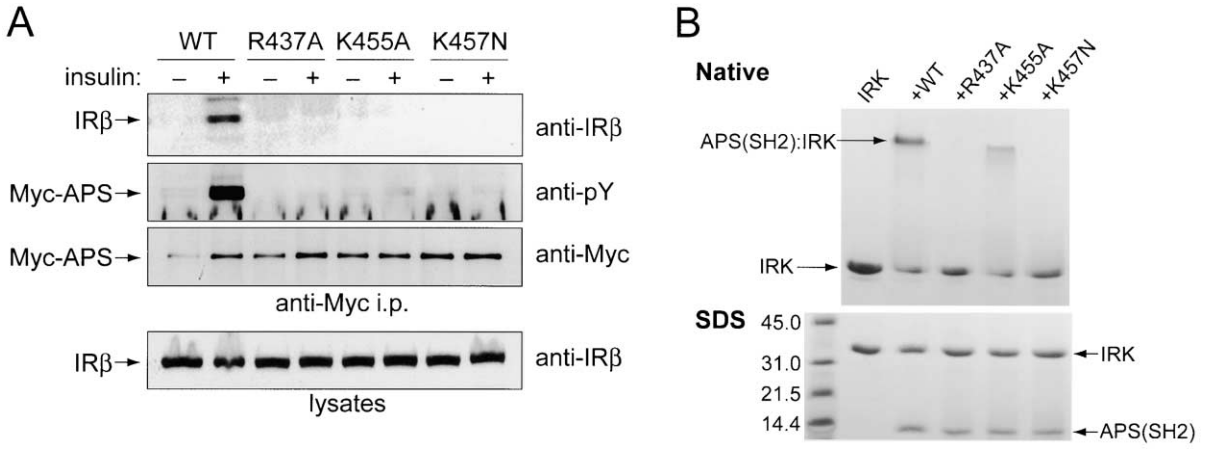

Figure 5. Mutagenesis of Basic Residues in the APS SH2 Domain that Interact with the IRK Activation Loop

(A) Mutagenesis of full-length APS in CHO-IR cells. Myc-tagged, full-length APS, either wild-type or mutants Arg-437→Ala, Lys-455→Ala, or Lys-457→Asn were transfected into CHO-IR cells. (Lys-457 was mutated to asparagine rather than alanine because the Lys-457→Ala SH2 domain as expressed in *E. coli* had poor solubility.) After treatment with or without 100 nM insulin, cells were lysed and immunoprecipitated with an anti-Myc antibody. Immunoprecipitates (top three blots) were analyzed by Western blotting using antibodies to the insulin receptor β subunit (top), to phosphotyrosine (middle), or to Myc (bottom). The lysates were analyzed by Western blotting using antibodies to the insulin receptor β subunit to show approximately equal amounts of insulin receptor in the lysates (bottom blot). The identification of the bands appears on the left side of the blots.

(B) Native gel-shift experiments with APS(SH2) mutants and IRK. Purified, tris-phosphorylated IRK (~15 μM) was mixed at an approximately 1:1 molar ratio with either purified, wild-type APS(SH2) (residues 401–504) or the APS(SH2) mutants Arg-437→Ala, Lys-455→Ala, or Lys-457→Asn. Samples were subjected to native PAGE (top) or SDS-PAGE (bottom, to show equal amounts of protein). In the native gel, tris-phosphorylated IRK alone migrates with high mobility (first lane), whereas APS(SH2) alone does not run into the native gel due to its high pI. The first lane contains IRK alone, and the second through fifth lanes contain IRK plus the indicated APS(SH2) protein. Complex formation between APS(SH2) and IRK is evident in the second lane (+WT) and to a lesser extent in the fourth lane (+K455A), and is absent in the third (+R437A) and fifth (+K457N) lanes. Molecular weight standards in kDa are shown on the left side of the SDS-PAGE gel.

sequence contexts) that reside outside of the core tyrosine kinase domain, e.g., the N-terminal juxtamembrane region. In contrast, APS is recruited via its SH2 domain to phosphotyrosines in the activation loop of the insulin receptor kinase domain (Ahmed et al., 1999; Moodie et al., 1999). RTKs contain one conserved tyrosine phosphorylation site in the activation loop (equivalent to Tyr-1163 in the insulin receptor), and either zero, one, or two additional sites, which suggests that these additional sites may serve a function other than enhancement of catalytic activity.

The insulin receptor contains three activation loop autophosphorylation sites, as do insulin-like growth factor-1 (IGF-1) receptor, TrkA/B/C, c-Met, MuSK, and c-Ros. APS is one of several proteins, including SH2-B (Kotani et al., 1998; Nelms et al., 1999) and Grb10 (Dong et al., 1997; He et al., 1998), that have been shown to bind to the phosphorylated activation loop of the insulin receptor. In most cases, the first phosphotyrosine in the activation loop, pTyr-1158, has been implicated as the site of interaction, which, along with pTyr-1162, is accessible (solvent exposed) in the crystal structure of the phosphorylated, activated form of IRK (Hubbard, 1997).

The sequence features of the IRK activation loop as a potential SH2 domain ligand are unusual: relative to pTyr-1158, an aspartate (Asp-1161) rather than a hydrophobic residue is found at the P+3 position and phosphotyrosines occupy the P+4 (pTyr-1162) and P+5 (pTyr-1163) positions. In addition, the phosphorylated activation loop (22 residues in IRK) is conformationally restricted, owing to multiple interactions between the activation loop and other kinase segments (Hubbard, 1997). To understand the structural basis for the interaction between the APS SH2 domain and the IRK activation loop, we determined a crystal structure of the APS(SH2)-IRK complex.

The crystal structure of the APS SH2 domain reveals a novel dimer in which the C-terminal half of each of the two protomers is reconfigured into an extended α helix (αB) of nearly twice the normal length. This helix, because of its position relative to the phosphotyrosine binding pocket of the other protomer within the dimer, will interfere with binding of phosphopeptides with the conventional, extended backbone conformation (Figure 1C).

Our structural and mutagenesis data demonstrate that Trp-475 (βF2) is a key determinant of APS(SH2) dimerization (Figures 1B and 4A). Based on the gel filtration results for the Trp-475→His substitution in APS(SH2) (Figure 4A), one would predict that the Lnk SH2 domain, which contains histidine at this position, is monomeric. Curiously, the SH2 domain of SH2-B also possesses a tryptophan at βF2, yet this SH2 domain is strictly monomeric (Figure 4A). Therefore, one or more residue differences between APS and SH2-B must destabilize dimer formation in the latter. For example, Val-479 in the APS SH2 structure is packed against the corresponding valine from the other protomer (Figure 1B). In SH2-B, isoleucine is found at this position (Figure 1D), which would be too bulky for optimal packing in the hydrophobic core. Indeed, a Val-479→Ile APS(SH2) mutant shows a reduced tendency to dimerize (data not shown).

Cotransfection experiments in COS-1 cells demonstrated that full-length APS associates with the APS

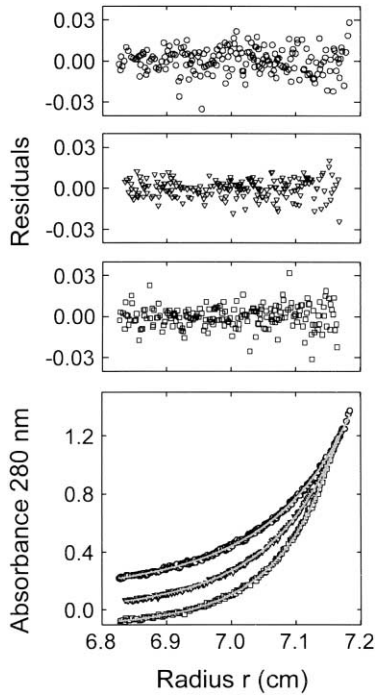

Figure 6. Binding of IRK to the APS SH2 Dimer Displays Negative Cooperativity

Sedimentation equilibrium profiles at 280 nm, and the corresponding residuals, for a 2:2 stoichiometric mixture of APS(SH2) and tris-phosphorylated IRK at a nominal loading concentration of 0.6 A_{280}. Symbols correspond to data collected at 14,000 (circles), 16,000 (triangles), and 18,000 (squares) rpm. The lines (gray) through the data represent best fits to reversible 2:1 and 2:2 APS(SH2):IRK complex formation. The fits yielded a K_d of 110 nM for binding of the first IRK molecule to the APS SH2 dimer, and a K_d of 160 μM for binding of the second IRK molecule to the 2:1 APS(SH2):IRK complex. For clarity, data collected at 14,000 rpm have been shifted by $+0.1$ A_{280}, whereas data collected at 18,000 rpm have been shifted by -0.1 A_{280}. The corresponding residuals for the fit are shown above the plot.

SH2 domain, providing evidence for the existence of a dimerized APS SH2 domain in the context of the full-length protein (Figure 4B). Similar experiments on SH2-B (Qian and Ginty, 2001) showed that full-length SH2-B and its SH2 domain do not associate, which is consistent with our finding that the SH2-B SH2 domain is monomeric (Figure 4A). That study also provided evidence for an oligomerization domain in the N-terminal region of SH2-B, which, based on secondary structure predictions, is also conserved in APS and Lnk. A second oligomerization region in APS would likely facilitate dimerization of its SH2 domain.

SH2 domains typically function as monomers. Interestingly, the Grb10 SH2 domain is also dimeric (Stein et al., 2003). In this case, the SH2 domain has canonical architecture, and the dimer interface comprises residues within and adjacent to αB. Based on conservation of the βD1 and βD3 lysines in Grb10 and SH2-B, one would predict that these adaptor proteins would also engage both pTyr-1158 and pTyr-1162 of the IRK activation loop. Versus the APS SH2 dimer, the monomeric SH2-B SH2 domain would be predicted to bind with reduced affinity and specificity, because of the greater solvent exposure of the βD3 lysine and the possibility of binding canonical phosphotyrosine ligands, respectively.

The APS SH2 domain has been shown to associate with RTKs other than the insulin receptor, including TrkA (Qian et al., 1998), the PDGF receptor (Yokouchi et al., 1999), and c-Kit (Wollberg et al., 2003). The APS SH2 domain interacts with TrkA via phosphotyrosines in the activation loop (Qian et al., 1998), presumably using the same mode of binding as described here for IRK; the two phosphotyrosines (pTyr-1158/1162) and two aspartates (Asp-1156/1161) in the IRK activation loop that interact with the APS SH2 domain are conserved in TrkA. These activation loop residues are also conserved in the IGF1 receptor and c-Ros, whereas MuSK and c-Met contain a substitution at either the first (to asparagine) or the second (to glutamate) aspartate, respectively, and lack the equivalent of Arg-1164 in the insulin receptor. Curiously, Wollberg et al. (2003) found that the APS SH2 domain binds to two phosphorylation sites in c-Kit, pTyr-568 (juxtamembrane region) and pTyr-936 (C-terminal tail), and that the interaction was dependent on a hydrophobic residue at the P+3 position, implying a canonical binding mode.

Sedimentation equilibrium experiments (Figure 6) revealed that the first IRK molecule binds to the APS SH2 dimer with relatively high affinity (100 nM range), whereas the second IRK molecule binds with significantly weaker affinity (100 μM range). Although the observed interactions with the activation loop are virtually the same for each of the two APS SH2 protomers, the N-terminal lobes of the two IRK molecules are separated by just 10 Å in the structure (Figure 2). Assuming a certain degree of flexibility in the docking of the first IRK onto the APS SH2 dimer, it is conceivable that the observed negative cooperativity derives from a partial IRK-IRK steric effect. Using the APS(SH2)-IRK structure as a rough spatial guide, the effective kinase concentration within an $\alpha_2\beta_2$ holoreceptor is estimated to be $\geq$1 mM, which would be more than sufficient to load both kinase domains onto the APS SH2 dimer. Negative cooperativity could possibly function to prevent APS-mediated dimerization of monomeric RTKs (e.g., TrkA) that have become phosphorylated in the absence of ligand.

The conformation of the phosphorylated activation loop is unchanged by APS(SH2) binding, indicating that the APS SH2 domain has evolved to bind efficiently to the conformation of the activation loop optimal for catalysis. Moreover, binding of the APS SH2 dimer to the two IRK activation loops leaves the substrate (ATP and peptide) binding sites accessible, as evidenced by the binding of the bisubstrate inhibitor to the complex (Figure 2). These recruitment features of the APS SH2 domain to the phosphorylated activation loop will facilitate phosphorylation of the C-terminal phosphorylation site in APS, Tyr-618, by the insulin receptor. Interestingly, recruitment of Cbl to pTyr-618 of APS requires dimerization of Cbl via its leucine zipper region (Liu et al., 2003), indicating that the 2-fold symmetry in the signaling complex (two β subunits, APS SH2 dimer) persists for at least one additional downstream signaling event.

Why does APS use the activation loop of the insulin

receptor as a recruitment site instead of a phosphotyrosine in a nonkinase segment, such as the juxtamembrane region or C-terminal tail? One plausible explanation is that binding of APS to the activation loop could sustain receptor activity by affording protection to the activation loop from tyrosine phosphatases such as PTP1B. In support of this hypothesis, a recent study demonstrated that in CHO cells overexpressing APS, insulin receptor phosphorylation levels were elevated and activation of ERK and Akt was prolonged (Ahmed and Pillay, 2003).

In conclusion, this study provides an atomic-resolution description of the recruitment of an SH2 domain-containing protein to an activated RTK. The crystal structure of the APS(SH2)-IRK complex reveals that the APS SH2 domain is a dimeric, quad phosphotyrosine binding module, which is recruited to the phosphorylated activation loops of the two insulin receptor β subunits. These structural and biochemical studies extend the known functional repertoire of the SH2 domain, the principal phosphotyrosine-recognition domain in cellular signaling pathways.

Experimental Procedures

Protein Expression and Purification

IRK was expressed in baculovirus-infected Sf9 insect cells, purified, and autophosphorylated in vitro as described previously (Hubbard, 1997). The APS SH2 domain was subcloned from full-length rat APS. Two constructs were engineered, one encoding residues 401–510 and a C-terminal truncation encoding residues 401–504. The construct for the SH2 domain of SH2-B was subcloned from the γ isoform of murine SH2-B (kindly provided by K. Nelms) and encodes residues 519–628, which corresponds in sequence to the 401–510 construct of rat APS(SH2). These constructs were inserted into expression vector pET14b (Novagen), which includes a thrombin-cleavable, N-terminal 6xHis-tag. After cleavage, four residues (GSHM) are present N-terminal to the start of the native sequence. Site-directed mutagenesis on the APS SH2 domain was performed using the QuickChange system (Stratagene). All constructs were verified by automated DNA sequencing.

APS and SH2-B constructs were transformed into *E. coli* strain BL21(DE3)pLysS, and cultures were grown in Luria broth media at 37°C to an OD 600 of 0.6. Protein expression was induced by addition of isopropyl-thiogalactopyranoside (IPTG, 0.5 mM final) for 12 hr at 19°C. Cells were harvested, resuspended in lysis buffer (50 mM Tris [pH 8.0], 300 mM NaCl, 0.1% Triton X-100, 2 μg/ml aprotinin, 50 μg/ml antipain, 1 μg/ml leupeptin, and 5 mM 2-mercaptoethanol), and lysed by French press. The lysate was centrifuged at 16,000 rpm for 1 hr and the supernatant was collected. The protein was isolated by Ni-NTA chromatography (Qiagen), cleaved by thrombin to remove the His-tag, and further purified by gel filtration chromatography (Superdex-75, Pharmacia).

To produce selenomethionyl-labeled APS(SH2), the pET14b plasmid encoding residues 401–510 was transformed into methionine-auxotrophic *E. coli* strain B834(DE3)pLysS. Cells were grown in Le-Master media containing seleno-L-methionine (Sigma) and Kao Michayluk vitamin solution (Sigma). The protein was purified similarly to the nonlabeled protein.

X-Ray Crystallography

Crystals of selenomethionyl-labeled APS(SH2), residues 401–504 (after thrombin cleavage), were grown at 4°C using the hanging drop vapor diffusion method. 1.0 μl APS(SH2) at 7 mg/ml was mixed with 0.5 μl reservoir buffer consisting of 1.4 M ammonium sulfate and 100 mM Tris (pH 7.5). Crystals belong to space group $P3_121$ with unit cell dimensions a=b=78.38 Å, c=67.33 Å. There is one APS SH2 dimer in the asymmetric unit with a solvent content of 51%. Data were collected at four wavelengths about the selenium K-edge (see Table 1) on beamline X4A at the National Synchrotron Light Source. Data were processed using DENZO/Scalepack (Otwinowski and Minor, 1997). The APS(SH2) structure was determined using SOLVE (Terwilliger and Berendzen, 1999), based on data at three wavelengths (peak, edge, remote; first three wavelengths in Table 1). Two well-ordered selenium sites were identified, in the two copies of (Se)Met-482 in the asymmetric unit. Maximum likelihood density modification and automated model building were performed with RESOLVE (Terwilliger, 2000). Data at the fourth wavelength (below the edge) were used in structure refinement. For the APS(SH2) and APS(SH2)-IRK structures, rigid-body refinement, simulated annealing, and positional and B factor refinement were performed with CNS (Brünger et al., 1998), and model building with O (Jones et al., 1991).

Tris-phosphorylated IRK and APS(SH2) (residues 401–504) were mixed in a 1:1.4 molar ratio and concentrated to ~10 mg/ml. Crystals were grown at 4°C in hanging drops containing 1.0 μl of protein solution [7 mg/ml of APS(SH2)-IRK complex, 0.33 mM of bisubstrate inhibitor, and 1 mM $MnCl_2$] and 1.0 μl of reservoir buffer (15% [w/v] polyethylene glycol [PEG] 8000, 100 mM HEPES [pH 8.0], 125 mM NaCl, 50 mM KH_2PO_4, and 3% [v/v] ethanol). The crystals belong to orthorhombic space group $P2_12_12_1$ with unit cell dimensions a=87.22 Å, b=96.44, and c=121.99 Å. There is one 2:2 complex in the asymmetric unit with a solvent content of 56%. Before being flash frozen in liquid propane, crystals were equilibrated in a series of stabilizing solutions with increasingly higher PEG 8000 concentration (2% increments from 15% to 25%), and subsequently transferred into cryosolvents that included 5%, 10%, 15%, then 20% ethylene glycol. Data were collected on beamline X25 at the National Synchrotron Light Source, and were processed using DENZO/Scalepack (Otwinowski and Minor, 1997). A molecular replacement solution was found with AMoRE (Navaza, 1994) using the structures of tris-phosphorylated IRK (Hubbard, 1997) and APS(SH2) as search models.

Sedimentation Equilibrium

Samples of the APS SH2 domain (residues 401–504) and tris-phosphorylated IRK were prepared in 400 mM NaCl, 50 mM HEPES (pH 8.0), and 5 mM 2-mercaptoethanol and studied at nominal loading concentrations of 0.5–0.6 A_{280}. Sedimentation equilibrium experiments were conducted at 4.0°C and rotor speeds of 16,000 to 22,000 rpm on a Beckman Optima XL-A analytical ultracentrifuge. Data were acquired as an average of 16 absorbance measurements at a nominal wavelength of 280 nm and a radial spacing of 0.001 cm. Equilibrium was achieved within 48 hr. Data were analyzed in terms of a single ideal solute to obtain the buoyant molecular mass, $M_1(1-v_1\rho)$, using the Optima XL-A data analysis software (Beckman). Values of M_1 were calculated using densities, ρ, obtained from standard tables and calculated v_1 values (Perkins, 1986).

2:1, 2:2, and 2:4 stoichiometric mixtures of the APS SH2 domain and tris-phosphorylated IRK were studied at nominal loading concentrations of 0.6 A_{280}. Data were collected at 4.0°C and rotor speeds of 14,000 to 18,000 rpm as above and analyzed in terms of reversible 2:1 and 2:2 APS(SH2):IRK complex formation, essentially as described previously (Shi et al., 1997). Similar experiments were carried out on a 2:2 stoichiometric mixture at a nominal loading concentration of 2.5 A_{280}, with data collected at 298 nm and analyzed as above.

Mammalian Cell Transfection, Immunoprecipitation, and Immunoblotting

Antibodies to hemagglutinin (HA) (F-7), Myc (9E10), and the insulin receptor β chain were purchased from Santa Cruz, Inc. The anti-phosphotyrosine monoclonal antibody (4G10) was from Upstate Biotechnology, Inc. Horseradish peroxidase-linked secondary antibodies were from Pierce Chemical Co. The Myc-tagged rat APS (pRK5-Myc-APS) construct was kindly provided by D. Ginty. APS cDNA, both full-length and the SH2 domain construct encoding residues 400–505, was derived from pRK5-Myc-APS by PCR. The triple HA-tagged APS was made by placing APS cDNA in frame in the BamH1 and EcoR1 sites of the pKH3 vector. Myc-tagged flotillin (residues 151–428) was constructed by placing mouse flotillin cDNA in frame in the BamH1 and Xho1 sites of pRK7-Myc. Point mutations in APS were generated by using the Stratagene QuickChange muta-

genesis kit, and the mutations were confirmed by automated DNA sequencing.

CHO-IR cells were maintained in α-minimal essential medium containing 10% fetal bovine serum. COS-1 cells were grown in Dulbecco's modified Eagle's medium (DMEM) containing 10% fetal bovine serum. Before insulin treatment, CHO-IR cells were serum deprived for 3 hr in F-12 Ham's medium. CHO-IR and COS-1 cells were transfected by electroporation and FuGene 6 reagent (Roche Diagnostics), respectively, as described previously (Liu et al., 2002). Cells in 60-mm-diameter dishes were washed twice with ice-cold phosphate-buffered saline and were lysed for 30 min at 4°C with buffer containing 50 mM Tris-HCl (pH 8.0), 135 mM NaCl, 1% Triton X-100, 1.0 mM EDTA, 1.0 mM sodium pyrophosphate, 1.0 mM sodium orthovanadate, 10 mM NaF, and protease inhibitors (one tablet per 7 ml of buffer) (Roche Diagnostics). The clarified lysates were incubated with the indicated antibodies for 1 hr at 4°C. The immune complexes were precipitated with protein A/G agarose (Santa Cruz Biotechnology, Inc.) for 1 hr at 4°C and were washed extensively with lysis buffer before solubilization in SDS sample buffer. Bound proteins were resolved by SDS-PAGE and transferred to nitrocellulose membranes. Individual proteins were detected with the specific antibodies and visualized by blotting with horseradish peroxidase-conjugated secondary antibodies.

Acknowledgments

We thank P. Cole for the bisubstrate inhibitor, Y. Lu and T. Neubert for mass spectrometry, M. Mohammadi for manuscript comments, and M. Becker and C. Ogata for support in synchrotron data collection. This work was supported by an American Diabetes Association research award (to S.R.H.) and National Institutes of Health grant DK060591 (to A.R.S.).

Received: July 3, 2003
Revised: September 24, 2003
Accepted: October 1, 2003
Published: December 18, 2003

References

Ahmed, Z., and Pillay, T.S. (2003). Adapter protein with a pleckstrin homology (PH) and an Src homology 2 (SH2) domain (APS) and SH2-B enhance insulin-receptor autophosphorylation, extracellular-signal-regulated kinase and phosphoinositide 3-kinase-dependent signalling. Biochem. J. *371*, 405–412.

Ahmed, Z., Smith, B.J., Kotani, K., Wilden, P., and Pillay, T.S. (1999). APS, an adapter protein with a PH and SH2 domain, is a substrate for the insulin receptor kinase. Biochem. J. *341*, 665–668.

Brünger, A.T., Adams, P.D., Clore, G.M., DeLano, W.L., Gros, P., Grosse-Kunstleve, R.W., Jiang, J.S., Kuszewski, J., Nilges, M., Pannu, N.S., et al. (1998). Crystallography & NMR system: a new software suite for macromolecular structure determination. Acta Crystallogr. D *54*, 905–921.

Chiang, S.H., Baumann, C.A., Kanzaki, M., Thurmond, D.C., Watson, R.T., Neudauer, C.L., Macara, I.G., Pessin, J.E., and Saltiel, A.R. (2001). Insulin-stimulated GLUT4 translocation requires the CAP-dependent activation of TC10. Nature *410*, 944–948.

Dong, L.Q., Farris, S., Christal, J., and Liu, F. (1997). Site-directed mutagenesis and yeast two-hybrid studies of the insulin and insulin-like growth factor-1 receptors: the Src homology-2 domain-containing protein hGrb10 binds to the autophosphorylated tyrosine residues in the kinase domain of the insulin receptor. Mol. Endocrinol. *11*, 1757–1765.

Ebina, Y., Ellis, L., Jarnagin, K., Edery, M., Graf, L., Clauser, E., Ou, J.H., Masiarz, F., Kan, Y.W., Goldfine, I.D., et al. (1985). The human insulin receptor cDNA: the structural basis for hormone-activated transmembrane signalling. Cell *40*, 747–758.

Eck, M.J., Shoelson, S.E., and Harrison, S.C. (1993). Recognition of a high-affinity phosphotyrosyl peptide by the Src homology-2 domain of p56lck. Nature *362*, 87–91.

He, W., Rose, D.W., Olefsky, J.M., and Gustafson, T.A. (1998). Grb10 interacts differentially with the insulin receptor, insulin-like growth factor I receptor, and epidermal growth factor receptor via the Grb10 Src homology 2 (SH2) domain and a second novel domain located between the pleckstrin homology and SH2 domains. J. Biol. Chem. *273*, 6860–6867.

Hendrickson, W.A. (1991). Determination of macromolecular structures from anomalous diffraction of synchrotron radiation. Science *254*, 51–58.

Hubbard, S.R. (1997). Crystal structure of the activated insulin receptor tyrosine kinase in complex with peptide substrate and ATP analog. EMBO J. *16*, 5572–5581.

Hubbard, S.R., and Till, J.H. (2000). Protein tyrosine kinase structure and function. Annu. Rev. Biochem. *69*, 373–398.

Jones, T.A., Zou, J.Y., Cowan, S.W., and Kjeldgaard, M. (1991). Improved methods for building protein models in electron density maps and the location of errors in these models. Acta Crystallogr. A *47*, 110–119.

Kotani, K., Wilden, P., and Pillay, T.S. (1998). SH2-Balpha is an insulin-receptor adapter protein and substrate that interacts with the activation loop of the insulin-receptor kinase. Biochem. J. *335*, 103–109.

Kuriyan, J., and Cowburn, D. (1997). Modular peptide recognition domains in eukaryotic signaling. Annu. Rev. Biophys. Biomol. Struct. *26*, 259–288.

Liu, J., Kimura, A., Baumann, C.A., and Saltiel, A.R. (2002). APS facilitates c-Cbl tyrosine phosphorylation and GLUT4 translocation in response to insulin in 3T3–L1 adipocytes. Mol. Cell. Biol. *22*, 3599–3609.

Liu, J., DeYoung, S.M., Hwang, J.B., O'Leary, E.E., and Saltiel, A.R. (2003). The roles of Cbl-b and c-Cbl in insulin-stimulated glucose transport. J. Biol. Chem. *278*, 36754–36762.

Moodie, S.A., Alleman-Sposeto, J., and Gustafson, T.A. (1999). Identification of the APS protein as a novel insulin receptor substrate. J. Biol. Chem. *274*, 11186–11193.

Navaza, J. (1994). AMoRe: an automated package for molecular replacement. Acta Crystallogr. A *50*, 157–163.

Nelms, K., O'Neill, T.J., Li, S., Hubbard, S.R., Gustafson, T.A., and Paul, W.E. (1999). Alternative splicing, gene localization, and binding of SH2-B to the insulin receptor kinase domain. Mamm. Genome *10*, 1160–1167.

Otwinowski, Z., and Minor, W. (1997). Processing of x-ray diffraction data collected in oscillation mode. Methods Enzymol. *276*, 307–326.

Parang, K., Till, J.H., Ablooglu, A.J., Kohanski, R.A., Hubbard, S.R., and Cole, P.A. (2001). Mechanism-based design of a protein kinase inhibitor. Nat. Struct. Biol. *8*, 37–41.

Perkins, S. (1986). Protein volumes and hydration effects. The calculations of partial specific volumes, neutron scattering matchpoints and 280-nm absorption coefficients for proteins and glycoproteins from amino acid sequences. Eur. J. Biochem. *15*, 169–180.

Qian, X., and Ginty, D.D. (2001). SH2-B and APS are multimeric adapters that augment TrkA signaling. Mol. Cell. Biol. *21*, 1613–1620.

Qian, X., Riccio, A., Zhang, Y., and Ginty, D.D. (1998). Identification and characterization of novel substrates of Trk receptors in developing neurons. Neuron *21*, 1017–1029.

Rahuel, J., Gay, B., Erdmann, D., Strauss, A., Garcia-Echeverria, C., Furet, P., Caravatti, G., Fretz, H., Schoepfer, J., and Grutter, M.G. (1996). Structural basis for specificity of Grb2–SH2 revealed by a novel ligand binding mode. Nat. Struct. Biol. *3*, 586–589.

Riedel, H., Wang, J., Hansen, H., and Yousaf, N. (1997). PSM, an insulin-dependent, pro-rich, PH, SH2 domain containing partner of the insulin receptor. J. Biochem. (Tokyo) *122*, 1105–1113.

Saltiel, A.R., and Pessin, J.E. (2002). Insulin signaling pathways in time and space. Trends Cell Biol. *12*, 65–71.

Shepherd, P.R., Withers, D.J., and Siddle, K. (1998). Phosphoinositide 3-kinase: the key switch mechanism in insulin signalling. Biochem. J. *333*, 471–490.

Shi, J., Ghirlando, R., Beavil, R.L., Beavil, A.J., Keown, M.B., Young, R.J., Owens, R.J., Sutton, B.J., and Gould, H.J. (1997). Interaction of the low-affinity receptor CD23/Fc epsilonRII lectin domain with

the Fc epsilon3–4 fragment of human immunoglobulin E. Biochemistry *36*, 2112–2122.

Stein, E.G., Ghirlando, R., and Hubbard, S.R. (2003). Structural basis for dimerization of the Grb10 Src homology 2 domain: implications for ligand specificity. J. Biol. Chem. *278*, 13257–13264.

Takaki, S., Watts, J.D., Forbush, K.A., Nguyen, N.T., Hayashi, J., Alberola-Ila, J., Aebersold, R., and Perlmutter, R.M. (1997). Characterization of Lnk. An adaptor protein expressed in lymphocytes. J. Biol. Chem. *272*, 14562–14570.

Terwilliger, T.C. (2000). Maximum-likelihood density modification. Acta Crystallogr. D Biol. Crystallogr.*56*, 965–972.

Terwilliger, T.C., and Berendzen, J. (1999). Automated MAD and MIR structure solution. Acta Crystallogr. D Biol. Crystallogr. *55*, 849–861.

Ullrich, A., Bell, J.R., Chen, E.Y., Herrera, R., Petruzzelli, L.M., Dull, T.J., Gray, A., Coussens, L., Liao, Y.C., Tsubokawa, M., et al. (1985). Human insulin receptor and its relationship to the tyrosine kinase family of oncogenes. Nature *313*, 756–761.

Waksman, G., Shoelson, S.E., Pant, N., Cowburn, D., and Kuriyan, J. (1993). Binding of a high affinity phosphotyrosyl peptide to the Src SH2 domain: crystal structures of the complexed and peptide-free forms. Cell *72*, 779–790.

White, M.F. (1998). The IRS-signalling system: a network of docking proteins that mediate insulin action. Mol. Cell. Biochem. *182*, 3–11.

Wollberg, P., Lennartsson, J., Gottfridsson, E., Yoshimura, A., and Ronnstrand, L. (2003). The adapter protein APS associates with the multifunctional docking sites Tyr-568 and Tyr-936 in c-Kit. Biochem. J. *370*, 1033–1038.

Yokouchi, M., Wakioka, T., Sakamoto, H., Yasukawa, H., Ohtsuka, S., Sasaki, A., Ohtsubo, M., Valius, M., Inoue, A., Komiya, S., and Yoshimura, A. (1999). APS, an adaptor protein containing PH and SH2 domains, is associated with the PDGF receptor and c-Cbl and inhibits PDGF-induced mitogenesis. Oncogene *18*, 759–767.

Accession Numbers

Coordinates and structure factors have been deposited in the Protein Data Bank with accession codes 1RPY for APS(SH2) and 1RQQ for APS(SH2)-IRK.